

THE ANOMALOUS X-RAY PULSAR 4U 0142+61: A NEUTRON STAR WITH A GASEOUS FALLBACK DISK

Ü. ERTAN,¹ M. H. ERKUT,¹ K. Y. EKŞİ,² AND M. A. ALPAR¹

Received 2006 June 7; accepted 2006 October 15

ABSTRACT

The recent detection of the anomalous X-ray pulsar (AXP) 4U 0142+61 in the mid-infrared with the *Spitzer* observatory by Z. Wang and coworkers constitutes the first instance of a disk around an AXP. We show, by analyzing earlier optical and near-IR data together with the recent data, that the overall broadband data set can be reproduced by a single model of an irradiated and viscously heated disk.

Subject headings: accretion, accretion disks — pulsars: individual (4U 0142+61) — stars: neutron — X-rays: bursts

1. INTRODUCTION

The zoo of young neutron stars contains a number of categories recognized by the distinct properties of such stars discovered or identified in the last decade. The existence of these different types of neutron stars strongly suggests that not all neutron stars are born with the same initial conditions, nor do they follow the same evolutionary path as the familiar radio pulsars, of which the typical young example is usually taken to be the Crab pulsar. Anomalous X-ray pulsars (AXPs) and soft gamma-ray repeaters (SGRs) (see Woods & Thompson 2005 for a review of AXPs and SGRs) are widely accepted to be magnetars (Duncan & Thompson 1992). The “radio-quiet” neutron stars (also known as central compact objects [CCOs]; Pavlov et al. 2004) and dim isolated (thermal) neutron stars (DTNs or DINs; Haberl 2005) are probably related classes, although the latter are relatively older. Measured rotation periods of AXPs, SGRs, and DINs cluster in the narrow range of 3–12 s. Alpar (2001) proposed that the presence or absence, and properties, of bound matter with angular momentum—that is, a fallback disk—may be among the initial parameters of newborn neutron stars, in addition to magnetic dipole moment and initial rotation rate. According to this scenario, the differences between isolated pulsars, AXPs, SGRs, and DINs, as well as the CCOs in certain supernova remnants, are due to different initial conditions, including the presence or absence and properties of fallback disks.

The suggestion that the X-ray luminosity of AXPs is due to mass accretion from a fallback disk (Chatterjee et al. 2000; Alpar 2001) has triggered searches for evidence of such disks. Searches for fallback disks around AXPs have been conducted primarily in the optical and near-IR bands. A realistic model for a putative fallback disk should take into account the effects of irradiation by the neutron star’s X-ray luminosity. Irradiation is the dominant source of disk luminosity for the outer disk at IR and longer wavelengths. The radial temperature profile of a fallback disk has been computed by Perna et al. (2000) and Hulleman et al. (2000) using the prescription given by Vrtilik et al. (1990). To estimate the temperatures, both Hulleman et al. and Perna et al. assumed the same particular irradiation efficiency and found that their estimated optical flux values lie well above the values indicated by observations of the AXPs 4U 0142+61 and 1E 2259+586. While

Perna et al. suggested that the difference might be due to a probable advection-dominated flow at the inner disk, Hulleman et al. drew the conclusion that this model can only fit the data for an unrealistically small outer disk radius and that fallback-disk models were ruled out (see § 4 for further discussion). Recent studies show that irradiated-disk model fits to existing detections and upper limits from AXPs allow the presence of accreting fallback disks with reasonable irradiation parameters for all AXPs (Ertan & Çalışkan 2006) when the fits are not restricted to a particular irradiation efficiency.

Recent results by Wang et al. (2006, hereafter WCK06) from *Spitzer* data on the AXP 4U 0142+61 complement earlier data in the near-infrared and optical (Hulleman et al. 2000, 2004, hereafter HvKK00 and HvKK04) and the detection of pulsed emission in the optical (Kern & Martin 2002), thus providing the first instance of a multiband data set that can be tested against disk models. WCK06 interpret their data with a dust disk radiating in the infrared, while the optical data are ascribed a magnetospheric origin. They take the origin of the X-ray luminosity to be dissipation of magnetic energy in the neutron star’s crust, in accordance with the standard magnetar model.

Here we show that the entire unpulsed optical, near-IR, and far-IR spectrum can be explained as due to a gaseous disk whose luminosity is provided by viscous energy dissipation due to mass transfer through the disk, as well as irradiation by the X-ray luminosity L_X from the neutron star. Taking L_X to be an accretion luminosity, as we do, links the irradiation contribution to the disk luminosity with the mass accretion rate \dot{M}_{acc} and, thereby, the mass inflow rate \dot{M} through the disk and the contribution of viscous dissipation to the disk luminosity. Luminosity in the optical band comes from the inner regions of the disk and is supplied, to a significant extent, although not fully, by the local viscous energy dissipation in the inner disk. The innermost disk, which is dominated by dissipation, radiates mostly in the UV band but also contributes to the total optical emission. Extension of the same irradiation model to outer regions of the disk explains the IR radiation. The disk luminosity is dominated by the contribution of irradiation at outer radii, where the thermal radiation peaks in the longer wavelength bands (see Table 1).

Pulsed emission in the optical (Kern & Martin 2002) is due to magnetospheric emission powered by a disk-shell dynamo in our model. It has been shown by Cheng & Ruderman (1991) that magnetospheric pulsar emission in optical and higher energy bands can be sustained by an outer gap in the presence of a disk

¹ Sabancı Üniversitesi, Orhanlı-Tuzla, Istanbul, Turkey.

² İstanbul Teknik Üniversitesi, Istanbul, Turkey.

protruding into the magnetosphere. This disk model is different from the first disk-magnetosphere models (Michel & Dessler 1981). More recently, Ertan & Cheng (2004) showed that the pulsed optical emission from 4U 0142+61 can be explained in terms of a magnetospheric model with a disk and a neutron star surface dipole magnetic field of $B_{\text{dipole}} \sim 10^{12}\text{--}10^{13}$ G. The magnetospheric emission is nearly 100% pulsed in this magnetosphere-disk model. The discovery of strongly pulsed optical emission (Kern & Martin 2002) has generally been perceived as excluding disk models, on the basis of the notion that magnetospheric emission cannot survive with a disk protruding into the light cylinder. The disk-magnetosphere model of Cheng & Ruderman (1991) and the application by Ertan & Cheng (2004) are important for fallback-disk models, since they demonstrate that a disk can actually be part of a magnetospheric mechanism that generates strongly pulsed emission.

The clustering of AXP and SGR rotational periods between 6 and 12 s was investigated by Psaltis & Miller (2002), who found that statistical clustering with a spin-down law of braking index $n \sim 2\text{--}4$ implies that the final period of these systems must be about 12 s. This final period does not correspond to reaching the “death line” in the $P\text{--}P$ plane, which reflects the cutoff voltage for magnetospheric emission. Within isolated dipole-magnetar models, the alternative possibility for reaching a final clustering period, asymptotically, is by magnetic field decay on timescales commensurate with the AXP and SGR ages (Psaltis & Miller 2002). An investigation of various magnetar field decay models (Colpi et al. 2000) has shown that having the X-ray luminosity data be associated with magnetic field decay is consistent with only one model, involving crustal Hall cascade, and for decay times less than about 10^4 yr. The presence of a fallback disk provides a natural explanation for period clustering of the AXPs (Chatterjee & Hernquist 2000), as well as dim isolated (thermal) neutron stars and SGRs (Alpar 2001; Ekşi & Alpar 2003). Fallback-disk models do not address the origin of bursts, while magnetar models explain the bursts by employing the energy stored in very strong magnetic fields. The basic workings of the magnetar models require only local magnetic stresses and energies in the neutron star crust, and they can thus be sustained with higher multipole components of the field, while the period clustering and explanation of torques with a fallback disk require the dipole component of the magnetic field to be on the order of $10^{12}\text{--}10^{13}$ G. Hybrid models (Ekşi & Alpar 2003; Ertan & Alpar 2003) with $B_{\text{multipole}} \sim 10^{14}\text{--}10^{15}$ G and $B_{\text{dipole}} \sim 10^{12}\text{--}10^{13}$ G are a possibility that incorporates a fallback disk.

In this paper, we evaluate the recent observations by WCK06 in conjunction with older results (§ 2). We show that the data agree quite well with a gaseous disk. In § 3, we estimate the characteristic lifetime of such a disk that has evolved through a propeller phase and find that the disk’s estimated age, depending on the torque model, is comparable to the $P_*/2\dot{P}_*$ characteristic age estimate taken as if dipole spin-down were effective. The discussion and conclusions are given in § 4.

2. INFRARED AND OPTICAL RADIATION FROM THE DISK AROUND 4U 0142+61

Recent *Spitzer* observations of the anomalous X-ray pulsar 4U 0142+61 have detected the source in the 4.5 and 8 μm infrared bands (WCK06). We will show that, taken together with the earlier observations in the optical (HvKK00, HvKK04; Morii et al. 2005), these detections are consistent with the presence of a gaseous disk around the neutron star. The optical detection must have a contribution from the magnetosphere, as implied by the

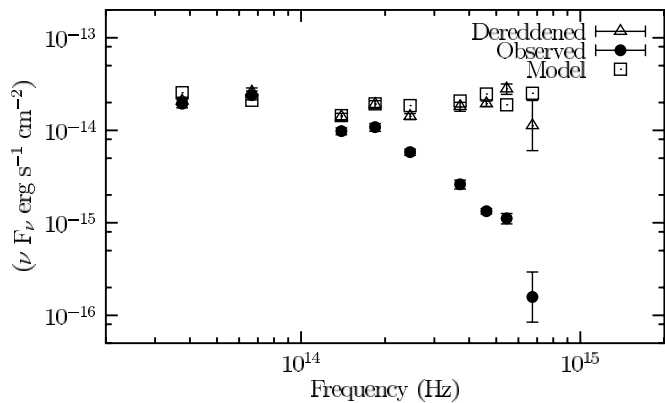


FIG. 1.—Energy flux data and irradiated-disk model values for 4U 0142+61 in the optical and infrared bands (B , V , R , I , J , H , K_s , 4.5 μm , and 8 μm). Circles are the observed (absorbed) data (taken from HvKK00 [V , R , I], HvKK04 [B , K_s], Morii et al. 2005 [H , J], and WCK06 [4.5 μm and 8 μm]), and triangles are data dereddened with $A_V = 3.5$. Squares are the irradiated-disk model energy flux values (see § 2).

strongly pulsed part of the optical signal, at 27% amplitude in the R band, observed by Kern & Martin (2002). Ertan & Cheng (2004) showed that the strongly pulsed emission from the magnetosphere can be accounted for either with a dipole-magnetar-based magnetosphere with surface dipole field strength $B_{\text{dipole}} \sim 10^{14}\text{--}10^{15}$ G or with a magnetosphere with a disk in it, with $B_{\text{dipole}} \sim 10^{12}\text{--}10^{13}$ G. The disk-magnetosphere model can provide nearly 100% pulsed magnetospheric emission in the optical. The presence of pulsed magnetospheric emission does not rule out the presence of a disk protruding into the magnetosphere. On the contrary, such a disk can be part of the magnetospheric circuit sustaining pulsed emission, as shown by Cheng & Ruderman (1991) and applied to 4U 0142+61 by Ertan & Cheng (2004). A pulsed component is likely to be present in the B , V , and IR bands. Uncertainties due to an unresolved pulsed fraction that is constant across the bands cannot be distinguished from uncertainties in other overall factors such as distance and disk inclination angle. Possible variations in the relative pulsed fractions in different bands should be taken into account in evaluating the model fits. Further, an important uncertainty arises from the interaction between inner disk and magnetosphere, which might distort the inner disk’s geometry and thus possibly lead to time-dependent self-shielding at some inner disk regions. Observations of various AXPs in some of the optical/IR bands at different epochs show considerable same-source variations in relative amplitudes (see, e.g., Morii et al. 2005). These variations are not included in our or other scientists’ model fits, and indeed, it is not feasible to model such effects in a plausible way. Keeping this in mind, we try to obtain the best fit to optical and IR data points.

Figure 1 shows the best model fit to all the data. Table 1 details the features of this fit. For each radiation band, the effective blackbody temperature representing that band and the radius R in the disk corresponding to that effective temperature are listed. The last column gives the ratio of dissipation- to irradiation-powered disk flux at that radius. The total emission in each band is predominantly supplied by parts of the disk near the quoted radius, but of course, there are lesser contributions from all parts of the disk. In the best fit displayed in Figure 1 and Table 1, the representative radius, 1×10^{10} cm, that dominates the V -band emission draws about 30% of its luminosity from viscous dissipation. The actual inner disk radius in this fit, $r_{\text{in}} = 10^9$ cm, is almost an order of magnitude smaller than the V -band representative radius. In the inner disk, the ratio of viscous dissipation to irradiation-supported flux

TABLE 1
MODEL TEMPERATURES AND RADII CORRESPONDING TO DIFFERENT
OPTICAL AND INFRARED BANDS

Band	T_{BB} (K)	R (cm)	D/F_{irr}
<i>B</i>	6516	7.0×10^9	0.45
<i>V</i>	5263	1.0×10^{10}	0.3
<i>R</i>	4454	1.4×10^{10}	0.30
<i>I</i>	3585	2.2×10^{10}	0.14
<i>J</i>	2377	4.8×10^{10}	0.07
<i>H</i>	1779	7.9×10^{10}	0.04
K_s	1324	1.4×10^{11}	0.02
$4.5 \mu\text{m}$	644	5.9×10^{11}	0.005
$8 \mu\text{m}$	362	1.9×10^{12}	0.002

NOTE.—The rightmost column shows the ratio of viscous dissipation rate to irradiation flux.

is therefore higher. The radiation from the innermost disk is a major contributor to the UV radiation bands. The innermost disk, from r_{in} to the *V*-band representative radius, also makes important contributions to the radiation in the optical bands. Therefore, the fits are quite sensitive to the value of the inner disk radius. The same disk model accommodates the earlier optical and IR data (HvKK00, HvKK04; Morii et al. 2005) and the *Spitzer* detections by WCK06. The value of A_V indicated by the best model fit shown in Figure 1 is 3.5. This is within the reasonable dereddening range $2.6 < A_V < 5.1$ for 4U 0142+61 (HvKK00, HvKK04) and coincides, fortuitously, with a recently derived estimate of $A_V = 3.5 \pm 0.4$ (Durant & van Kerkwijk 2006). For this model, all the model flux values remain within $\sim 30\%$ of the data points. The error bars on the *B*-band data point give the 3σ upper limit (HvKK04). Considering the uncertainties discussed above, the irradiated gaseous disk model is in reasonable agreement with optical and IR data.

In the inner disk, viscous dissipation contributes significantly to the disk luminosity, while in the outer and cooler parts of the disk, the luminosity is determined by X-ray irradiation from the neutron star. Notably, the total disk luminosity of a gaseous disk, including both irradiation and the intrinsic dissipation, does not fall off in the optical range in the way expected for a dust disk as employed by WCK06 in their Figure 3. Indeed, a gas disk model can explain both the optical and the IR data, as shown in Figure 1. The earlier conclusion by HvKK00 that an accretion disk is ruled out is no longer valid given the *Spitzer* observations. These authors ruled out an accretion disk because their optical magnitude, dereddened with $A_V = 5.4$, does not fall on the disk curve corresponding to L_X as an accretion luminosity, with certain assumptions, a choice of \dot{M} , and a particular irradiation reprocessing efficiency. Fitting the optical points to the Rayleigh-Jeans end of a disk blackbody therefore required, on the basis of the (only optical and near-IR) data then existing, that any disk in 4U 0142+61 be truncated at a certain outer radius r_{out} . Now, with the new *Spitzer* observations of WCK06, the disk is actually detected in the far-infrared. We can fit all the data in the optical and IR bands *B*, *V*, *R*, *I*, *J*, *H*, K_s , $4.5 \mu\text{m}$, and $8 \mu\text{m}$ (Fig. 1). A gaseous disk emitting in this energy range extends from an inner disk radius $r_{\text{in}} \simeq 1 \times 10^9$ cm to an outer radius of about 10^{12} cm (see Table 1). The two mid-IR *Spitzer* data points put a lower limit on the outer disk radius of around 10^{12} cm, but they do not constrain the extension of the outer disk beyond 10^{12} cm. In our model, the outer disk radius is $r_{\text{out}} = 2 \times 10^{12}$ cm. The quality of the fits does not change for even larger values of r_{out} , since the contribution to the *Spitzer* bands at 4.5 and $8 \mu\text{m}$ from larger radii is not significant.

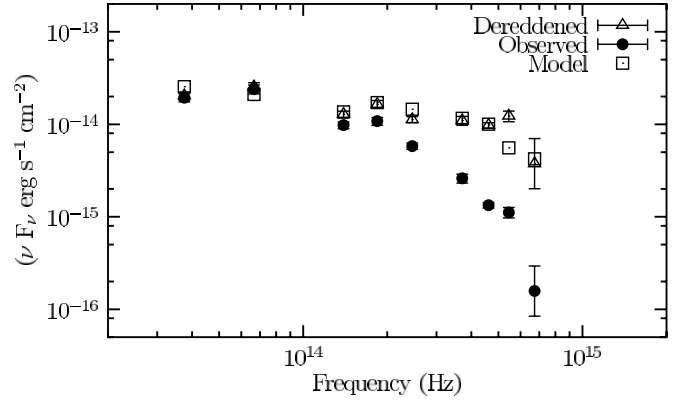


FIG. 2.—Same as Fig. 1, but with dereddening of $A_V = 2.6$ (triangles).

The model fits in the optical band are sensitive to the value of the disk's inner radius. This is taken to be the Alfvén radius,

$$r_{\text{in}} \simeq r_A \simeq f_1 \dot{M}^{-2/7} (GM_*)^{-1/7} \mu_*^{4/7}, \quad (1)$$

where M_* is the mass and μ_* is the dipole magnetic moment of the neutron star. The factor $f_1 \sim 0.5-1$ describes the uncertainty in the precise location of the inner radius. The mass inflow rate \dot{M} in the disk is larger than or equal to the mass accretion rate derived from the X-ray luminosity,

$$\dot{M}_{\text{acc}} \equiv \frac{L_X R_*}{GM_*} \equiv f_2 \dot{M} \leq \dot{M}, \quad (2)$$

where R_* is the radius of the neutron star. As the star is spinning down while accreting, it must be in the propeller regime but close to rotational equilibrium with the disk, according to the fallback-disk model (Alpar 2001). Some of the mass inflow through the disk may not be accreting under these circumstances. From the observed X-ray luminosity of $L_X \simeq 10^{35}$ ergs s^{-1} , taking $R_* = 10^6$ cm and $M_* = 1.4 M_\odot$ we obtain $\dot{M}_{\text{acc}} \simeq 5 \times 10^{14}$ g s^{-1} , which is related to the mass inflow rate \dot{M} , depending on the choice of f_2 . We first report model fits with $\dot{M} = \dot{M}_{\text{acc}}$ ($f_2 = 1$) and discuss modifications of the results for $(f_1, f_2) < 1$ in § 4. For a given \dot{M} , the inner radius depends on the strength of the dipole magnetic moment of the neutron star.

We calculate the radial effective temperature profile $T_{\text{eff}}(r)$ considering both the disk surface flux due to the intrinsic viscous dissipation rate D of the disk,

$$D = \frac{3}{8\pi} \frac{GM_* \dot{M}}{r^3} \quad (3)$$

(see, e.g., Frank et al. 2002), and the irradiation flux,

$$F_{\text{irr}} = C \frac{\dot{M}_{\text{acc}} c^2}{4\pi r^2} \quad (4)$$

(Shakura & Sunyaev 1973), where the irradiation parameter C includes the effects of disk geometry, albedo of the disk surface, and the conversion efficiency of the mass accretion into X-rays. In our calculations, we take C to be constant along the disk and leave its value as a free parameter. For comparison with the data, we integrate the disk blackbody emission in each of the optical and IR observational bands (see Ertan & Çalışkan 2006 for details of calculations). The model energy flux values presented in Figures 1 and 2 were obtained with $C = 1 \times 10^{-4}$. While the irradiation geometry of AXP disks might be somewhat different from

those of low-mass X-ray binary (LMXB) disks (Ertan et al. 2006; Ertan & Çalışkan 2006), the values of C that we find in our fits lie in the range expected for LMXBs ($\sim 10^{-4}$ to 10^{-3}), in particular, based on disk stability analyses of soft X-ray transients (de Jong et al. 1996; Dubus et al. 1999; Ertan & Alpar 2002). With C 's in this range, the optical/IR observations for the other three AXPs with available data can also be fitted with disk models with irradiation and viscous dissipation (Ertan & Çalışkan 2006).

In Figures 1 and 2, we present two different model fits. Figure 1 shows the best fit, obtained with $A_V = 3.5$, with the dipole field at the neutron star's surface set to be 10^{12} G on the equator (2×10^{12} G at the poles). After these fits were made, we learned of work on X-ray and optical extinction and reddening (Durant & van Kerkwijk 2006) reporting $A_V = 3.5 \pm 0.4$ for 4U 0142+61. The inner disk radius r_{in} for the model in Figure 1 is 10^9 cm. The model fits are comparable for values of r_{in} up to a few times 10^9 cm, with smaller r_{in} corresponding to larger A_V . The corotation radius for 4U 0142+61 is $r_{\text{co}} \simeq 7 \times 10^8$ cm, which is near the inner disk radius we obtain from the best model fit. This implies that the system is indeed near rotational equilibrium. The system is in the propeller regime, as indicated by the spin-down of the AXP. Nevertheless, most or all of the inflowing disk matter is being accreted onto the neutron star rather than being effectively propelled out of the system, on account of the closeness to equilibrium. This is consistent with our model fits obtained with the assumption that $f_2 = 1$.

The largest value of the dipole magnetic field allowed by the model fits corresponds to the lowest value of A_V . For the direction of 4U 0142+61, reasonable values of the dereddening in the direction of the AXP lie in the range $2.6 < A_V < 5.1$ (HvKK00, HvKK04). Figure 2 shows the model fit for the largest value of the magnetic dipole field. This was obtained by setting $A_V = 2.6$, the minimum value in the range considered, and allowing a 60% discrepancy in the V band. Note that the discrepancy in V is $\sim 30\%$ for the best fit, with $A_V = 3.5$. The inner radius of the disk is $r_{\text{in}} = 8 \times 10^9$ cm. The corresponding dipole magnetic field value is found to be 2×10^{13} G on the equator (4×10^{13} G at the poles). The disk model fits preclude higher values of the dipole component of the magnetic field. A stronger dipole field, $B_* > 10^{14}$ G, would cut the disk at much larger radii, above 10^{10} cm. This is not consistent with the optical (R , V , B) data.

In comparing dereddened fluxes with models for various values of B_{dipole} and A_V , we find that the highest discrepancies always occur in the V band, where the dereddened fluxes are always somewhat larger than the model predictions. In the B band, the observations have yielded only an upper limit. Predictions in the B band from models that fit the V , R , and IR bands are consistent with this upper limit.

3. LIFETIME OF THE DISK AROUND 4U 0142+61

Could a fallback disk remain active, exerting a torque on the neutron star, at the age of 4U 0142+61? In this section, we explore the evolution of the disk under various models for the torque between the disk and the neutron star. The characteristic lifetime of a fallback disk around a propeller can be estimated as $\tau_d = M_d/\dot{M}$, where \dot{M} is the mass inflow rate in the disk. For a steady configuration, the disk's mass-loss rate is $\dot{M}_d = -\dot{M}$. The mass-loss rate \dot{M}_d will include the accretion rate \dot{M}_{acc} onto the neutron star, as well as \dot{M}_{out} , the mass lost from the disk–neutron star system. In an effective propeller situation, \dot{M}_{out} may make up most of \dot{M}_d . As the outer radius of the disk is not constrained by the data, the disk mass cannot be calculated from the fits. Instead, we shall assume plausible values, consistent with the observed disk to within an order of magnitude. We then use torque models to es-

timate the mass inflow rate \dot{M} through the disk from the observed spin-down rate $\dot{\Omega}_*$.

The long-term spin history of a rapidly rotating magnetized neutron star depends on the types of torques acting on it. The net torque on a magnetized neutron star interacting with an accretion disk can be expressed in general as

$$N_* \equiv I_* \dot{\Omega}_* = j \dot{M} (GM_* r_{\text{in}})^{1/2}, \quad (5)$$

where j is the nondimensional torque as a function of the fastness parameter $\omega_* \equiv \Omega_*/\Omega_K(r_{\text{in}})$, Ω_* being the angular spin frequency of the neutron star, r_{in} the inner disk radius, $\Omega_K = (GM_*/r^3)^{1/2}$ the Keplerian angular velocity, and I_* the moment of inertia of the neutron star. Using the observed value of $\dot{\Omega}_*$ in equation (5), we estimate the mass inflow rate as

$$\dot{M}_{17} \simeq 0.4 \omega_*^{-1/3} |j|^{-1} P_*^{-7/3} I_{*,45} \times \left(\frac{\dot{P}_*}{10^{-12} \text{ s s}^{-1}} \right) \left(\frac{M_*}{1.4 M_\odot} \right)^{-2/3}, \quad (6)$$

where \dot{M}_{17} is the mass inflow rate in units of 10^{17} g s^{-1} , $I_{*,45}$ is the neutron star's moment of inertia in units of 10^{45} g cm^2 , and $P_* = 2\pi/\Omega_*$ is the spin period of the neutron star (Erkut & Alpar 2004).

In earlier epochs of its evolution, an AXP with a fallback disk is likely to be in the propeller phase, in which the neutron star is rotating rapidly with respect to the rotation rates in the inner boundary of the disk. Most or all of the mass supplied by the disk is lost from the system rather than being accreted by the propeller neutron star. This goes on until the neutron star has spun down to rotation rates close to corotation with the disk. When the star rotates only a little faster than the inner disk, a significant fraction of the mass lost by the disk may be accreted onto the neutron star while, at the same time, the star is spinning down under torques applied by the disk.

The propeller-type spin-down torque first considered by Illarionov & Sunyaev (1975) scales as $|N_1| \sim (\mu_*^2/r_A^3)\Omega_K(r_A)/\Omega_*$ (see Ghosh 1995). Depending on the spin rate of the neutron star as compared with the sound speed at the magnetospheric boundary, the scaling of the braking torques for subsonic and supersonic propellers are given by $|N_2| \sim \mu_*^2 \Omega_*^2 / GM_*$ and $|N_3| \sim \mu_*^2 \Omega_* \Omega_K(r_A) / GM_*$, respectively (Davies & Pringle 1981; Ghosh 1995). In these models, the magnetospheric radius is the Alfvén radius (see eq. [1]). The spin-down torque for a subsonic propeller, N_2 , is independent of \dot{M} and not used in the present work. The torques N_1 and N_3 can be expressed as in equation (5) with $j = -\omega_*^q$, where $q = -1$ and $q = 1$ for N_1 and N_3 , respectively. The braking torque considered by Wang & Robertson (N_4 ; 1985) has the same form as N_3 , but with a particular estimate for the inner radius of the disk in the propeller stage, that is, $N_4 = -\omega_* \dot{M} (GM_* r_{\text{in}})^{1/2}$, where $r_{\text{in}} = 2^{-3/16} \Omega_*^{-3/8} \dot{M}^{-1/8} (2GM_*)^{1/8} \mu_*^{1/4}$. This scaling of the inner disk radius is simply that of the Alfvén radius when $r_{\text{in}} = r_A = r_{\text{co}} \equiv (GM_*/\Omega_*^2)^{1/3}$, the corotation radius. All the braking torques yield the same \dot{M} when $\omega_* = 1$, in other words, when $r_{\text{in}} = r_{\text{co}}$.

We now estimate the lifetime of a fallback disk around 4U 0142+61 using these different types of propeller torque for disks of mass $M_d = 10^{-6} M_\odot$ and $M_d = 10^{-5} M_\odot$. For each torque model, solving equation (6) with the implicit \dot{M} - and B_* -dependence of ω_* and $j(\omega_*)$ gives the current value of the mass inflow rate \dot{M} . For $M_d = 10^{-6} M_\odot$, the inferred values for the lifetime of the disk around 4U 0142+61 corresponding to the propeller torques N_1 , N_3 , and N_4 can be written for $R_* = 10^6$ cm and

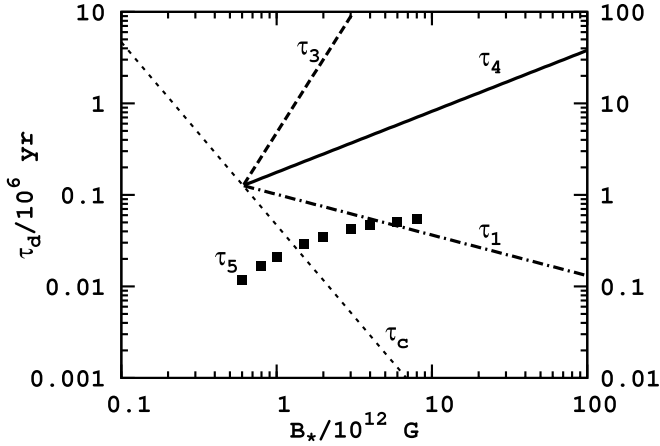


FIG. 3.—Disk lifetime as a function of stellar magnetic field strength for different propeller torques. Squares show the disk lifetime values estimated from the spin-down torque N_5 in the accretion regime. The left vertical axis shows the estimated lifetime range for a disk of mass $M_d = 10^{-6} M_\odot$. The vertical axis at right is for $M_d = 10^{-5} M_\odot$.

$M_* = 1.4 M_\odot$ as $\tau_1 \simeq 1.0 \times 10^5 B_{*,12}^{-4/9}$ yr, $\tau_3 \simeq 4.8 \times 10^5 B_{*,12}^{8/3}$ yr, and $\tau_4 \simeq 1.8 \times 10^5 B_{*,12}^{2/3}$ yr, respectively, where $B_{*,12}$ is the surface dipole magnetic field strength on the poles of the neutron star in units of 10^{12} G. For $M_d = 10^{-5} M_\odot$, all age estimates are greater by a factor of 10. In the initial life of the neutron star, after a brief initial accretion phase the propeller regime will start when $r_{\text{in}} > r_{\text{co}}$ and will prevail until the inner radius reaches the corotation radius again. As the inner radius of the disk r_{in} approaches r_{co} , the propeller regime will allow accretion. For all torque models, the condition $r_{\text{in}} = r_{\text{co}}$ yields the same mass inflow rate,

$$\dot{M} = \Omega_*^{7/3} (GM_*)^{-5/3} \mu_*^2, \quad (7)$$

which yields for $M_d = 10^{-6} M_\odot$ the critical age estimate

$$\tau_c \simeq 4.67 \times 10^4 B_{*,12}^{-2} \text{ yr}. \quad (8)$$

As shown in Figure 3, τ_c is the minimum estimated lifetime for a fallback disk if the neutron star is spinning down under the action of propeller torques without accreting any matter onto its surface. In our model, the AXPs experience propeller spin-down (with some accretion) when $r_{\text{in}} \geq r_{\text{co}}$. The characteristic ages τ_i of the disk estimated from the propeller torques N_1 , N_3 , and N_4 are greater than τ_c when $r_{\text{in}} > r_{\text{co}}$, depending on the value of B_* . Figure 3 shows that the present age estimate is larger than τ_c for all of the torques considered here if the magnetic dipole field strength on the poles is greater than 6×10^{11} G. If the end of the propeller phase is taken to occur when $r_{\text{in}} = r_A = r_{\text{co}}$, as commonly assumed and adopted by WCK06, then $B_{*,12} \simeq 0.6$ is obtained with $\tau_c \simeq 1.3 \times 10^5 \text{ yr} = \tau_1 = \tau_3 = \tau_4$ for $M_d = 10^{-6} M_\odot$ and $\tau_c \simeq 1.3 \times 10^6 \text{ yr} = \tau_1 = \tau_3 = \tau_4$ for $M_d = 10^{-5} M_\odot$ (see Fig. 3).

In scenarios with these propeller torques N_1 , N_3 , and N_4 , 4U 0142+61 must have spent most of its lifetime in the propeller phase with little or no accretion, and it must have entered its current phase of spin-down with accretion more recently. In the past, all or most of the incoming disk matter would have been thrown out of the system as envisaged in the original propeller scenario (Illarionov & Sunyaev 1975). While in the present stage the gas disk is supplying the X-ray luminosity of 4U 0142+61 by accretion, in the past the X-ray luminosity was supplied not primarily by accretion but by some other mechanism, such as dis-

sipation of the magnetic field in the neutron star's surface, as in magnetar models (Thompson & Duncan 1995), or by internal energy dissipation in the neutron star, as expected for neutron stars under torques but without initial cooling or accretion as a dominant source of surface thermal luminosity (Alpar et al. 1984; Alpar 2001).

If, on the other hand, there is accretion onto the neutron star over some parts of its surface while a fraction of the infalling disk matter escapes from the stellar magnetosphere as outflow or wind (see Illarionov & Kompaneets 1990), the torque is given by

$$N_5 = -\dot{M}_{\text{out}} \Omega_* r_{\text{in}}^2 + \dot{M}_{\text{acc}} \Omega_K(r_{\text{in}}) r_{\text{in}}^2, \quad (9)$$

where $\dot{M}_{\text{out}} = \dot{M} - \dot{M}_{\text{acc}}$ by conservation of mass, with the mass accretion rate, $\dot{M}_{\text{acc}} = L_X R_* / GM_*$, expressed in terms of the X-ray luminosity L_X . We have defined the mass outflow rate \dot{M}_{out} and the accretion rate \dot{M}_{acc} as positive quantities. When the negative propeller torque described by the first term dominates, the net torque N_5 acts to spin down the neutron star. Such a spin-down phase allows one to explain the persistent-stage L_X of AXPs and SGRs with partial accretion from a fallback disk, as we have done here. The first term in equation (9) is the braking torque on the neutron star due to mass loss when $\dot{M}_{\text{out}} < 0$ (Ghosh 1995). The second term represents the angular momentum flux onto the neutron star due to accreting disk matter. If accretion of matter onto the neutron star has already started by a switching off of the effective propeller mechanism within the recent history of 4U 0142+61, we would expect to find commensurate estimates of age and magnetic field strength based on both N_5 and one of the propeller torques N_1 , N_3 , and N_4 , whichever is an apt description of the actual torque effective in the system's past. In Figure 3, we plot the age and polar surface magnetic field strength estimates from N_1 , N_3 , N_4 , and N_5 . Note that the spin-down torque N_5 and the propeller torque N_1 yield a common estimate ($B_* \sim 6 \times 10^{12}$ G) for the dipolar component of the magnetic field. Even for the smaller disk mass ($M_d = 10^{-6} M_\odot$), the torque models N_3 and N_4 produce very large ages for $B_* > 10^{12}$ G. The torque N_5 represents the most plausible model, because it incorporates accretion with spin-down and yields reasonable ages, together with the torque N_1 , for $B_{\text{dipole}} \sim 10^{12} - 10^{13}$ G.

Using the observed parameters of 4U 0142+61 and torque N_5 , the mass inflow rate in the disk, for a given magnetic field strength, can be estimated from equation (9) along with the outflow rate \dot{M}_{out} . We find $\dot{M} \simeq 1.9 \times 10^{-11} M_\odot \text{ yr}^{-1}$ and $\dot{M}_{\text{out}} \simeq 3 \times 10^{-12} M_\odot \text{ yr}^{-1}$ for $B_* = 6 \times 10^{12}$ G and $\dot{M}_{\text{acc}} \simeq 1.6 \times 10^{-11} M_\odot \text{ yr}^{-1}$ ($\sim 10^{15} \text{ g s}^{-1}$). Note that most of the mass lost by the disk accretes onto the neutron star. This estimate implies $f_2 = 0.85$ for $f_1 = 1$.

The upper limit set on the lifetime of the disk by employing N_5 is much smaller than the lifetime values estimated using the propeller torques N_3 and N_4 . The spin-down age of the pulsar estimated with the dipole spin-down formula, which of course can only offer a rough comparison with the present model, $P_*/2\dot{P}_* \sim 10^5 \text{ yr}$, is comparable to τ_5 , the inferred disk lifetime corresponding to the spin-down torque N_5 in the accretion regime (see Fig. 3). This age estimate is also consistent with those for the supernova remnants associated with the AXPs 1E 2259+586 and 1E 1841-045. We conclude that an active disk torquing down the star for an age of $\sim 10^5 \text{ yr}$ is a tenable hypothesis, most likely with some accretion for a significant part of its history up to the present.

With the assumption that N_5 is a good description of the current torque, one can estimate the fraction f_2 of the mass inflow that is accreted, for a given value of the disk inner radius, without

having prior knowledge of the mass inflow rate in the disk. Equation (9) can be written in the form

$$\frac{\dot{M}_{\text{out}}}{\dot{M}_{\text{acc}}} = \left(\frac{r_{\text{co}}}{r_{\text{in}}}\right)^{3/2} + \frac{I_* |\dot{\Omega}_*|}{\dot{M}_{\text{acc}} \Omega_* r_{\text{in}}^2}, \quad (10)$$

where we have substituted $N_5 = I_* |\dot{\Omega}_*|$. Using the observed spin-down rate and the accretion rate inferred from the luminosity (eq. [2]), we find $f_2 = 0.6$ for $r_{\text{in}} = 10^9$ cm and $f_2 = 0.4$ for $r_{\text{in}} = r_{\text{co}} = 7 \times 10^8$ cm.

4. DISCUSSION AND CONCLUSIONS

By combining earlier optical data (HvKK00, HvKK04; Morii et al. 2005) with recent *Spitzer* infrared data (WCK06), we have shown that the full data set is consistent with the luminosity and spectrum expected from a gas disk. The optical radiation is powered to a significant extent by viscous dissipation in the inner regions of the disk, while the IR radiation comes from outer regions where irradiation by the central source is the primary source of the disk's local luminosity.

What is the maximum dipole magnetic moment μ_* that is compatible with these disk model fits to the data? From equations (1) and (2), we obtain

$$\mu_* = f_1^{-7/4} f_2^{-1/2} r_{\text{in}}^{7/4} \dot{M}_{\text{acc}}^{1/2} (GM_*)^{1/4}. \quad (11)$$

Using $f_1 = 0.5$ and $f_2 = 1.0$ and employing the maximum $r_{\text{in}} \simeq 8 \times 10^9$ cm that is compatible with our fits, for a minimum $A_V = 2.6$ we find the maximum possible μ_* to be 5.8×10^{31} G cm³, corresponding to a maximum surface dipole field of 1.2×10^{14} G on the poles of a neutron star of mass $1.4 M_\odot$ and radius $R_* = 10^6$ cm. A further increase in the upper limit for the magnetic field can be obtained with smaller values of f_2 . The minimum f_2 that allows a fit within 60% *V*-band deviation is around 0.3, together with $r_{\text{in}} \simeq 1.0 \times 10^{10}$ cm. For these extremes of parameter values, we obtain $B_* \simeq 3 \times 10^{14}$ G on the pole of the neutron star. These estimates should be noted together with the uncertainties due to disk-magnetosphere interaction, possible shielding effects, and time-dependent variations, as discussed in § 2.

We note that if the disk inner radius is large, $r_{\text{in}} \gg r_{\text{co}}$, the neutron star is a fast rotator, far from rotational equilibrium with the disk, and likely to be in the strong-propeller regime. If the simple description of propeller spin-down given by equation (9) is roughly correct, as is likely the case, the large moment arm provided by a large r_{in} , together with mass outflows at least comparable to (and probably larger than) the mass accretion rate onto the star will yield spin-down rates much larger than that observed:

$$|\dot{\Omega}_*| \sim \dot{M}_{\text{acc}} \Omega_* r_{\text{in}}^2. \quad (12)$$

A disk with $r_{\text{in}} \simeq 1.0 \times 10^{10}$ cm, which allows for a magnetic dipole as large as $B_* \simeq 3 \times 10^{14}$ G, requires a spin-down rate of $|\dot{\Omega}_*| \sim 10^{-10}$ rad s⁻². This is much larger than the observed $|\dot{\Omega}_*| \simeq 1.7 \times 10^{-13}$ rad s⁻². Here we have a strong indication against values of r_{in} large enough accommodate dipole magnetic fields in the magnetar range.

As our disk models depend only on the mass inflow rate \dot{M} inside the disk and the irradiation parameter C , it could be argued that the entire mass inflow actually turns into an outflow and none of the mass flowing through the disk is accreted onto the neutron star, the X-ray luminosity being due to some energy-release mech-

anism other than accretion. The observation that the inner disk radius in our best fit is so close to the corotation radius argues against this. Indeed, our fits yield the inner radius required by the optical observations. The actual inner radius may be even smaller and closer to r_{co} , but we do not have the possibility of observing such a highly absorbed source in the UV band to check. The rather small value of the spin-down rate compared with what one would expect with a substantial mass outflow from a larger inner radius also indicates that this is a weak propeller, close to equilibrium. It is therefore likely that there is mass accretion.

Could the disk of our model fits be passive, with no viscous dissipation, no mass inflow, and no accretion at all onto the neutron star? Under this hypothesis, the disk luminosity would be generated entirely by irradiation by the neutron star's X-ray luminosity, which in turn is not due to accretion. It is unlikely that there is no accretion at all, if there is a gas disk with the properties indicated by our model fits, which are sensitive to the inner disk radius and require temperatures above 10^5 K in the inner disk. The disk cannot be neutral and passive at these temperatures; it has to be ionized, whether it is pure hydrogen or contains heavy elements. An ionized disk would have viscosity generated by the magnetorotational instability (Balbus & Hawley 1991), which will result in mass inflow through the disk and interaction between the disk and the neutron star magnetosphere, as well as some mass accretion onto the neutron star, depending on the closeness to equilibrium. Ionization temperatures for hydrogen disks are on the order of 6000 K. For fallback disks with heavy metals (Werner et al. 2007), the ionization temperatures could be as low as ~ 2500 K. In hydrogen-disk simulations of soft X-ray transients and dwarf novae, two different viscosity parameters are employed, above and below the ionization temperatures, to account for the observations of these systems. In these models, the viscosity parameter decreases by a factor of 0.01–0.5 as the temperatures decrease to below the ionization temperature T_i . This indicates that even the disk regions with $T < T_i$ remain active and that the critical temperature below which the entire disk enters a passive state is likely to be much lower than the ionization temperatures. Early studies by Gammie (1996) on protoplanetary disks suggested the possibility that a weakly ionized disk might become passive in its dense regions in the midplane while accretion proceeds over its surface. Recent work by Inutsuka & Sano (2005), however, indicates the existence of various physical mechanisms that can provide, sustain, and homogenize a sufficient degree of ionization for the magnetorotational instability (MRI) to work through most regions of a protoplanetary disk even at temperatures as low as 300 K. According to Inutsuka & Sano, once MHD turbulence starts to prevail in a disk, it seems quite difficult to switch it off. The state of turbulent viscosity keeps the temperature and other parameters such that the ionization level required for MRI is self-sustained.

The presence of the disk imposes constraints only on the dipole component of the magnetic field. The very strong magnetic fields that are employed to explain SGR and AXP bursts in the magnetar model may well reside in the higher multipole structure of the neutron star's surface magnetic field. In this hybrid situation, dissipation of the magnetar fields' energy in the neutron star crust may contribute to the surface luminosity along with accretion. In this case, \dot{M}_{acc} will have a value less than that inferred by taking the X-ray luminosity to be fully due to accretion, as in equation (2).

The object 4U 0142+61 is the anomalous X-ray pulsar with the most detailed optical and IR observations. It would be of great interest to check and extend the current database with further observations, in particular with *Spitzer*. It is important to realize that

magnetar fields in higher multipoles and a dipole field with $B_* \lesssim 10^{13}$ G, to accommodate a disk with the equilibrium period range of observed period clustering, can coexist in a neutron star. The search for disks in other AXPs has also provided some data in the optical and near-infrared that are consistent with gas disk models, as discussed in Ertan & Çalıřkan (2006). Time-dependent variations in the X-ray luminosity could be smeared out during the X-ray reprocessing at the outer disk. On the other hand, variations in the mass inflow rate modify the disk emission in the optical bands before the changes have been observed in X-rays, because of varying accretion rates. Any observed signatures in the optical bands followed by similar variations in X-rays with viscous time delays (minutes to days) would be a clear indication of ongoing disk accretion onto the neutron star. At present, 4U 0142+61 seems to be the best source with which to test this idea.

Finally, we comment on the passive dust-disk model proposed by Wang et al. (2006). Their detection of 4U 0142+61 in the mid-infrared has firmly indicated, for the first time, the presence of a disk around an isolated neutron star. They fitted the data with a two-component model, using a power law to fit the optical and near-IR data, which they ascribe to magnetospheric emission.

This leaves only their recent discovery, the *Spitzer* detections in the mid-IR band, to be explained by a disk. Hence, while the evidence in that band clearly points to a disk, the association of only this narrowband emission with the disk constrains it to be a dust disk beyond the magnetosphere. Questions arising from this model concern why this disk did not generate some viscosity to extend into an active gaseous disk, how it cooled and remained cold and confined, and whether it is stable against the radiation pressure of the pulsar. With an inner disk radius $r_{\text{in}} \sim 2r_{\text{lc}}$, where r_{lc} is the light cylinder's radius, such a passive dust disk could be stable against the radiation pressure of the magnetospheric pulsar emission (Ekşi & Alpar 2005). This stability is valid for $r_{\text{lc}} \lesssim r_{\text{in}} \lesssim 2r_{\text{lc}}$ for orthogonal rotators and for even a wider range for non-orthogonal rotators, according to the investigation of Ekşi & Alpar (2005). The stability issue should be kept in mind for dust disks beyond the light cylinder.

We acknowledge research support from the Sabancı University Astrophysics and Space Forum. M. A. A. acknowledges support from the Turkish Academy of Sciences.

REFERENCES

- Alpar, M. A. 2001, *ApJ*, 554, 1245
 Alpar, M. A., Anderson, P. W., Pines, D., & Shaham, J. 1984, *ApJ*, 276, 325
 Balbus, S. A., & Hawley, J. F. 1991, *ApJ*, 376, 214
 Chatterjee, P., & Hernquist, L. 2000, *ApJ*, 543, 368
 Chatterjee, P., Hernquist, L., & Narayan, R. 2000, *ApJ*, 534, 373
 Cheng, K. S., & Ruderman, M. 1991, *ApJ*, 373, 187
 Colpi, M., Geppert, U., & Page, D. 2000, *ApJ*, 529, L29
 Davies, R. E., & Pringle, J. E. 1981, *MNRAS*, 196, 209
 de Jong, J. A., van Paradijs, J., & Augusteijn, T. 1996, *A&A*, 314, 484
 Dubus, G., Lasota, J.-P., Hameury, J.-M., & Charles, P. 1999, *MNRAS*, 303, 139
 Duncan, R. C., & Thompson, C. 1992, *ApJ*, 392, L9
 Durant, M., & van Kerkwijk, M. H. 2006, *ApJ*, 650, 1082
 Ekşi, K. Y., & Alpar, M. A. 2003, *ApJ*, 599, 450
 ———. 2005, *ApJ*, 620, 390
 Erkut, M. H., & Alpar, M. A. 2004, *ApJ*, 617, 461
 Ertan, Ü., & Alpar, M. A. 2002, *A&A*, 393, 205
 ———. 2003, *ApJ*, 593, L93
 Ertan, Ü., & Çalıřkan, Ş. 2006, *ApJ*, 649, L87
 Ertan, Ü., & Cheng, K. S. 2004, *ApJ*, 605, 840
 Ertan, Ü., Göğüş, E., & Alpar, M. A. 2006, *ApJ*, 640, 435
 Frank, J., King, A., & Raine, D. 2002, *Accretion Power in Astrophysics* (3rd ed.; Cambridge: Cambridge Univ. Press)
 Gammie, C. F. 1996, *ApJ*, 457, 355
 Ghosh, P. 1995, *J. Astrophys. Astron.*, 16, 289
 Haberl, F. 2005, in *Five Years of Science with XMM-Newton*, ed. U. G. Briel, S. Sembay, & A. Read (MPE Rep. 288) (Garching: MPI extraterr. Phys.), 39
 Hulleman, F., van Kerkwijk, M. H., & Kulkarni, S. R. 2000, *Nature*, 408, 689 (HvKK00)
 ———. 2004, *A&A*, 416, 1037 (HvKK04)
 Illarionov, A. F., & Kompaneets, D. A. 1990, *MNRAS*, 247, 219
 Illarionov, A. F., & Sunyaev, R. A. 1975, *A&A*, 39, 185
 Inutsuka, S., & Sano, T. 2005, *ApJ*, 628, L155
 Kern, B., & Martin, C. 2002, *Nature*, 417, 527
 Michel, F. C., & Dessler, A. J. 1981, *ApJ*, 251, 654
 Morii, M., Kawai, N., Kataoka, J., Yatsu, Y., Kobayashi, N., & Terada, H. 2005, *Adv. Space Res.*, 35, 1177
 Pavlov, G. G., Sanwal, D., & Teter, M. A. 2004, in *IAU Symp. 218, Young Neutron Stars and Their Environments*, ed. F. Camilo & B. M. Gaensler (San Francisco: ASP), 239
 Perna, R., Hernquist, L., & Narayan, R. 2000, *ApJ*, 541, 344
 Psaltis, D., & Miller, M. C. 2002, *ApJ*, 578, 325
 Shakura, N. I., & Sunyaev, R. A. 1973, *A&A*, 24, 337
 Thompson, C., & Duncan, R. C. 1995, *MNRAS*, 275, 255
 Vrřilek, S. D., Raymond, J. C., Garcia, M. R., Verbunt, F., Hasinger, G., & Kürster, M. 1990, *A&A*, 235, 162
 Wang, Y.-M., & Robertson, J. A. 1985, *A&A*, 151, 361
 Wang, Z., Chakrabarty, D., & Kaplan, D. L. 2006, *Nature*, 440, 772 (WCK06)
 Werner, K., Nagel, T., & Rauch, T. 2007, *Ap&SS*, in press (astro-ph/0608529)
 Woods, P. M., & Thompson, C. 2005, in *Compact Stellar X-Ray Sources*, ed. W. H. G. Lewin & M. van der Klis (Cambridge: Cambridge Univ. Press), 547